The Abdus Salam
International Centre for Theoretical Physics

United Nations
Educational, Scientific
and Cultural Organization

International Atomic
Energy Agency

SMR 1673/8

AUTUMN COLLEGE ON PLASMA PHYSICS

5 - 30 September 2005

On the Theory of Plasma-Wall Transition Layer

D. Tskhakaya
University of Innsbruck, Austria

ON THE THEORY OF PLASMA-WALL TRANSITION LAYER

D.D. Tskhakaya sr.[1,2], K.-U. Riemann[3], P.K. Shukla[3], B. Eliasson[3],

J. Seebacher[1], S. Kuhn[1]

[1] *Department of Theoretical Physics, University of Innsbruck, A-6020 Innsbruck, Austria.*
[2] I*nstitute of Physiucs, Georgian Academy of Sciences, 0177 Tbilisi, Georgia.*
[3] *Institute for Theoretical Physics, Ruhr-University, D-44780 Bochum, Germany.*

Abstract

The problem of the plasma-wall transition (PWT) layer in an unmagnetized plasma is considered.

In the first part of the lecture, a self-consistent two-scale formalism is presented and the asymptotic ($\lambda_D/\lambda \to 0$, where λ_D is the electron Debye length and λ is the ion mean free path) presheath and sheath solutions are analyzed for the well-known hydrodynamic Tonks-Langmuir PWT model: a plasma, consisting of Boltzmann-distributed electrons and singly charged ions, is enclosed by two absorbing negatively charged walls. The ion gas, described in the hydrodynamic approximation, is assumed to be collision-free. On the scale of the (quasi-neutral) presheath, the sheath edge is distinguished as a singular point of the electric field, whereas on the scale of the (non-neutral) sheath it is defined by the boundary condition of vanishing electric field. At the sheath edge the Bohm criterion is fulfilled in the marginal (equality) form. The problem of matching the presheath and sheath solutions is closely related to the consistent analysis of the transition region near the sheath edge. Introducing an "intermediate scale", for small but finite ratios λ_D/λ, the presheath and sheath solutions can be matched smoothly. The eigenvalue problem originating from the plasma balance (the ion loss to the wall must be balanced by the ion production due to electron-neutral ionization collisions) is considered.

In the second part of the lecture, the problem of the PWT layer in a semibounded plasma is considered whithout explicit splitting into sheath and presheath regions. The ion dynamics is described by kinetic theory and includes ionization, recombination and charge-exchange collisions. A condition is derived which must be fulfilled by the ion velocity throughout the whole PWT layer in order to exclude oscillatory behaviour of the electrostatic potential. The resulting system of equations is solved numerically. A comparison of recent experimental results with a numerical solution of model presented here reveals that the model accurately describes the transition from the bulk plasma to the wall.

The lecture is mainly based on the results of the following papers:

1. *The plasma-sheath matching problem in the hydrodynamic Tonks-Langmuir model,*
K.-U. Riemann, J. Seebacher, D.D. Tskhakaya sr., and S. Kuhn (submitted to Plasma Physics and Controlled Fusion).

2. *On the theory of plasma-wall transition layers,*
D.D. Tskhakaya sr, B. Eliasson, P.K. Shukla and S. Kuhn, Phys. Plasmas **11,** 3945 (2004).

1. Introduction

When a plasma is in contact with a surface, such as an electrode or a wall (e.g. in laboratory discharges), the surface typically becomes negatively charged due to the absorption of fast moving electrons. The negatively charged surface repels electrons and attracts ions which are pulled towards the surface [1]. This gives rise to charge separation near the surface, resulting in a strong electric field. The problem of the plasma boundary layer is one of the oldest issues in Plasma Physics. In the past, several investigations [2, 3, 4, 5] have dealt with this problem, and recent experiments in weakly collisional plasmas [6] have been conducted and their results compared with the theoretical predictions [7]. However, the problem of the plasma-wall transition (PWT) layer is still the subject of numerous investigations and violent controversies [8, 9, 10, 11]. This is due to the mathematical and physical difficulties related to the various competing nonlinear effects and boundary conditions.

The plasma is shielded from the wall by a thin positive space-charge layer ("sheath"), extending over several electron Debye lengths λ_{Ds}. Usually the Debye length is small compared with l_{ps} - the relevant length scale of the presheath. Here $\lambda_{Ds}(=\left[T_{es}/\left(4\pi n_{es}e^2\right)\right]^{1/2})$ is the Debye length at the "sheath edge" or "sheath entrance" (indicated by the subscript s) . Pioneers like Langmuir [12] and Bohm [13] used the plasma-sheath concept more or less intuitively. A strict mathematical justification based on an asymptotic, $\varepsilon = \lambda_{Ds}/l_{ps} \to 0$, two-scale formalism was developed in [2]. During the last decades, the analysis of PWT layers on the basis of the two-scale formalism was refined and extended to different complex conditions (see [5, 14] and references cited there).

In the "asymptotic two-scale approximation" usually employed, the PWT layer is split into two distinctly different sublayers, namely the collisional, quasi-neutral "preshath" and the collisionless, non-neutral "sheath" adjacent to the wall [5, 14], [16]. It can be shown that for $\varepsilon \to 0$ in a fluid description

$$u_i(z) \geqslant c(z) = \sqrt{\left(T_{es}^*(z) + \gamma_{is}T_{is}(z)\right)/m_i} \tag{1}$$

(the "fluid Bohm criterion") must be satisfied in the entire sheath region, where $u_i(z)$ is the ion fluid velocity, $c(z)$ is the ion sound speed, $T_e^* = en_e/\left[dn_e\left(\varphi\right)/d\varphi\right]^{-1}$ is the "electron screening temperature", T_i is the ion temperature, γ_i is the ion "polytropic" coefficient, m_i is the ion mass, $\varphi(z)$ is the electrostatic potential, and $n_e\left(\varphi\right)$ is the electron density. Temperatures are given in energetic units. The inequality sign in (1) holds inside the sheath, whereas the equality sign applies as a limit at the sheath edge (the "marginal fluid Bohm criterion"), dictating that the ions enter the sheath with the ion sound velocity $u_{is} = c_s = \sqrt{\left(T_{es}^* + \gamma_{is}T_{is}\right)/m_i}$. The criterion (1), which in its original, strongly simplified form

$$u_i \geqslant c_s = \sqrt{T_e/m_i}, \tag{2}$$

was given by Bohm [13], ensures the potential distribution to be spatially non-oscillatory at the sheath edge.n

The asymptotic two-scale approach allows one to avoid many of the mathematical difficulties associated with more realistic situations characterized by finite ε. The main potential drop takes place in the sheath, whereas a residual electric field penetrates into the presheath and accelerates the ions to the velocity c_s, required by the marginal Bohm criterion at the sheath entrance. The relevant presheath scale length l_{ps}, which is the minimum of the various collision mean-free paths (mfp) (ionization mfp λ_{ion} and recombination mfp λ_{rec} for electrons, ion mfp for charge-exchange collisions with neutrals λ_{exc}, etc.) and the curvature radius R [14], is assumed to be much larger than the Debye length. The asymptotic two-scale formalism implies neglecting the space charge on the presheath scale (in the presheath region, the quasineutrality condition holds) and collisions in the sheath region. In reality, however, the parameter ε defined above, is always finite and the asyptotic two-scale approach may be expected to yield reasonable results only if $\varepsilon \ll 1$. A common approach to take this into acocunt is to find separate solutions

for the presheath and sheath regions and join them in the "intermediate" region, i.e., in the transition region between the presheath and the sheath [14, 8, 17]. At a first glance there is no "region of common validity" representing the presheath-sheath interface. The asymptotic, $\varepsilon \to 0$, preshath solution runs into a electric field singularity, $\lambda_{ion}\, d\varphi/dz \to \infty$, at the sheath edge indicating that the subsequent sheath is infinitity thin on the presheath scale z/l_{ps} . On the sheath scale z/λ_{Ds}, in contrast, the presheath is infinitely remote and, consequently, the sheath edge is characterized by a zero electric field, $\lambda_{Ds}\, d\varphi/dz \to 0$. The seeming incompatibility can be resolved by reanalyzing the problem on an "intermediate scale" accounting in lowest order both for space charge and collision effects. This reanalysis requires to introduse a transition layer (inermediate region), which connects the presheath and sheath regions and fills in the region, where the presheath and sheath solutions differs from the exact solution. This procedure is called the matching of the asymptotic two-scale solutions. It consists in (i) matching the presheath solution with the intermediate solution and (ii) matching the intermediate solution with the sheath solution.

Below we consider matching of solutions for the hydrodynamic version of the plane Tonks-Langmuir model of the PWT layer: an one-dimensional collision-free plasma enclosed by two parallel absorbing walls. In fact there is no need to specify the plasma model in detail, because the mathematical description of the presheath-sheath transition is *universal* [14]*;* in particular it makes no difference whether the presheath effect is based on geometry, collisions, or ionization. For various reasons, however, it is convenient to investigate the hydrodynamic Tonks-Langmuir model:

(a) first, this simple model is most suitable to exhibit and clarify the specific difficulties originating from the coupling of the presheath-sheath analysis with the plasma eigenvalue problem. Physically the eigenvalue problem reflects the fact that the ion production rate due to electron-neutral ionization collisions must be equal to the rate at which ions are lost on the wall ("plasma balance"). For a given boundary condition (by prescribing the wall potential φ_w) the ionization frequency and the plasma dimension acquire a mutual dependence.

(b) second, the model is widely known and the asymptotic presheath solution is analytically known.

Hence, the asyptotic two-scale formalism implicitly needs the smallness of the parameter ε, $\varepsilon \ll 1$. While such an approximation may have its merits if ε is still sufficiently small, an unified treatment would be preferable both for fundamental scientific correctness and also for practical applications when ε can no longer be considered to be very small.

Below we present such a unified treatment. We investigate a PWT layer considering it as one unit, without *a priori* splitting it into presheath and sheath regions. For the ions we use a self-consistent kinetic treatment including ionization, recombination and charge-exchange collisions. The spatial dependences of the electron and ion densities, the ion velocity, and the electrostatic potential are investigated both analytically and numerically. A comparison of our numerical results with recent experimental observations [6] reveals exellent quantitative agreement, This experimental confirmation allows us to conclude that our model and the related assumptions describe the PWT layer correctly even in parameter regions where simplified models fails.

In addition, we formulate a general condition which must be satisfied throughout the whole PWT layer to ensure spatially non-oscillatory solutions even when the ion velocity goes to zero far away from the wall (i.e., at distances $\gtrsim l_{ps}$).

Tonks-Langmuir model of PWT layer

2. Basic Equations

The famous plane symmetric discharge model of Tonks and Langmuir describes a collisionless plasma in front of two absorbing walls. Because of the symmetry of the system with respect to the midplane $z = 0$ it is sufficient to investigate the half space occupied by plasma, $0 \le z \le L$. The cold fluid approach of the plane problem leads to the following dimensionless set of equations [3],[13]

$$\begin{aligned} \frac{d}{dy}(nu) &= \frac{L\sigma}{c_s}e^{-\phi} \\ u\frac{du}{dy} &= -\frac{d\phi}{dy} - \frac{L\sigma}{c_s}\frac{u}{n}e^{-\phi} \\ \left(\frac{\lambda_D}{L}\right)^2 \frac{d^2\phi}{dy^2} &= n - e^{-\phi} \end{aligned} \tag{3}$$

where $\phi = -e\varphi/T_e$ is the potential, $n_- = e^{-\phi}$ represents the normalized electron density $n_- = n_e/n_e(0)$, $n = n_i/n_e(0)$ designates the dimensionless ion density, and $u = v_i/c_s = v_i/\sqrt{T_e/M_i}$ denotes the dimensionless ion flow velocity. The natural way to normalize the space coordinate z would be to normalize it with the dimension of the plasma, which is for the Tonks-Langmuir model the distance L from the plasma center to the wall. In this case we normalize $y = z/L$ and obtain (3). The ionization frequency σ is a left open parameter which is not known a priori. It has to be determined from the solution of the problem, and is therefore an eigenvalue of the problem. This ionization frequency σ and the dimension of the plasma vessel L have a mutual dependency, which physically reflects the so called plasma balance. It says that the rate, at which ions are lost on the wall, must be equal to the ion production rate. For a given length L the ionization frequency has to adjust to this length in the stationary case. A solution procedure of (3) is shown in [3] but it is rather complicated. A more convenient way is to set $L\sigma/c_s = 1$ and to normalize z in the following way - $x = \sigma z/c_s$ (the presheath scale), which leads to the system of equations

$$\begin{aligned} \frac{d}{dx}(nu) &= e^{-\phi} \\ u\frac{du}{dx} &= \frac{d\phi}{dx} - \frac{u}{n}e^{-\phi} \\ \varepsilon^2\frac{d^2\phi}{dx^2} &= n - e^{-\phi} \end{aligned} \tag{4}$$

Now the length L becomes an eigenvalue of the problem and the wall position is not known a priori. The common way to find a solution of (4) is to start the calculation at the plasma center and to proceed until the boundary condition, $\varphi = \varphi_w$,at the wall is fulfilled (φ_w is the potential on the wall). The distance L from the plasma center to the wall can be determined afterwards as a result of the calculation. Eqs. (4) contain only one parameter $\epsilon = \lambda_D/\lambda$ with the Debye length λ_D $(= \left[T_e/\left(4\pi e^2 n_e(0)\right)\right]^{1/2})$ and $\lambda = c_s/\sigma$. The length λ is said to be the plasma presheath scale, because in fact it characterizes the length from the plasma center to the sheath edge, which will be defined later. So in this case $\lambda \equiv l_{ps}$ (see the Introduction). The parameter ε is called the smallness parameter because in most applications $\varepsilon \ll 1$. From this fact it becomes clear why we can apply perturbation theory to find at least approximate solutions. But Eqs.(4) represent a singular perturbation problem, because in the limit $\varepsilon \to 0$ the highest derivative in (4) vanishes, and it is not possible to fulfill the boundary conditions at the wall. From perturbation theory we know that another scale can be defined which is called the sheath (inner) scale via $\xi = (z - z_r)/\lambda_D = (x - x_r)/\varepsilon$, which leads to

$$\begin{aligned} \frac{d}{d\xi}(nu) &= \varepsilon e^{-\phi} \\ \frac{d}{d\xi}\left(\frac{u^2}{2} - \phi\right) &= \varepsilon e^{-\phi}\frac{u}{n} \\ \frac{d^2\phi}{d\xi^2} &= n - e^{-\phi}. \end{aligned} \tag{5}$$

The constant z_r(or x_r) is arbitrary, but later we will see, that it can be used to adjust the position of the sheath. It should be mentioned that the sheath cannot be related to the wall in our calculation because the wall position is not known.
From the physical point of view there is no difference between (4) and (5), we have only changed the normalization of the space coordinate. Solutions can be found numerically. The results for (4) are demonstrated for different values of ε in Fig.1.

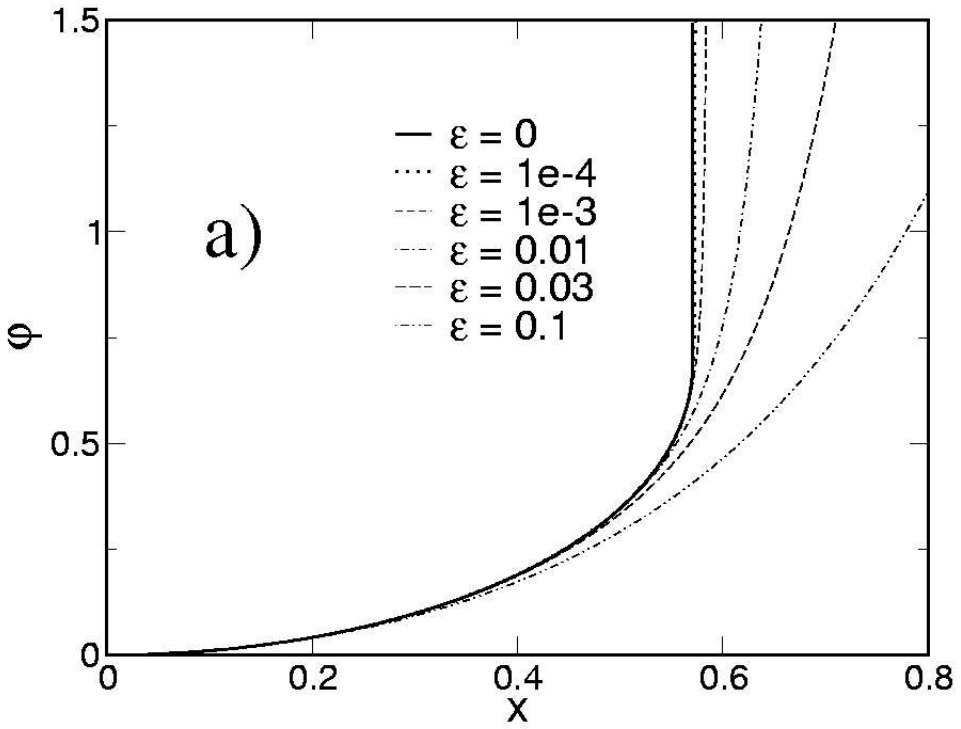

Figure 1: Normalized potential curves for the plane Tonks-Langmuir model with finite ϵ on the presheath scale.

One observes that the plasma region is resolved well on presheath scale but the sheath region is not clearly visible to the observer. On the other hand the same solutions on the sheath scale look quite different, as demonstrated in Fig.2. Now the gradients in the sheath region are clearly visible. On both scales it is not possible to determine a distinct point where the presheath ends and the sheath begins, which makes it difficult to distinguish a presheath region and a sheath region.

To overcome this difficulty it is possible to introduce a third scale, which is called the intermediate scale, with $\zeta = (z - z_s)/l_m = (x - x_s)/\delta$, where $l_m = \lambda_D^{4/5}\lambda^{1/5}$ and $\delta = \epsilon^{4/5}$. In Fig.3 there are plotted again the same results as shown in Fig.1 and in Fig.2, but now on this intermediate scale. One observes a region where the curves for different values of ε has a common range of validity. In principle there is no distinct point which separates the presheath from the sheath, but the common region of the different solutions shown in Fig.3 gives a reasonable hint where the plasma ends and the sheath begins.

3. Asymptotic Analysis of the Presheath and Sheath scales

3.1 Asymptotic Presheath Scale Analysis

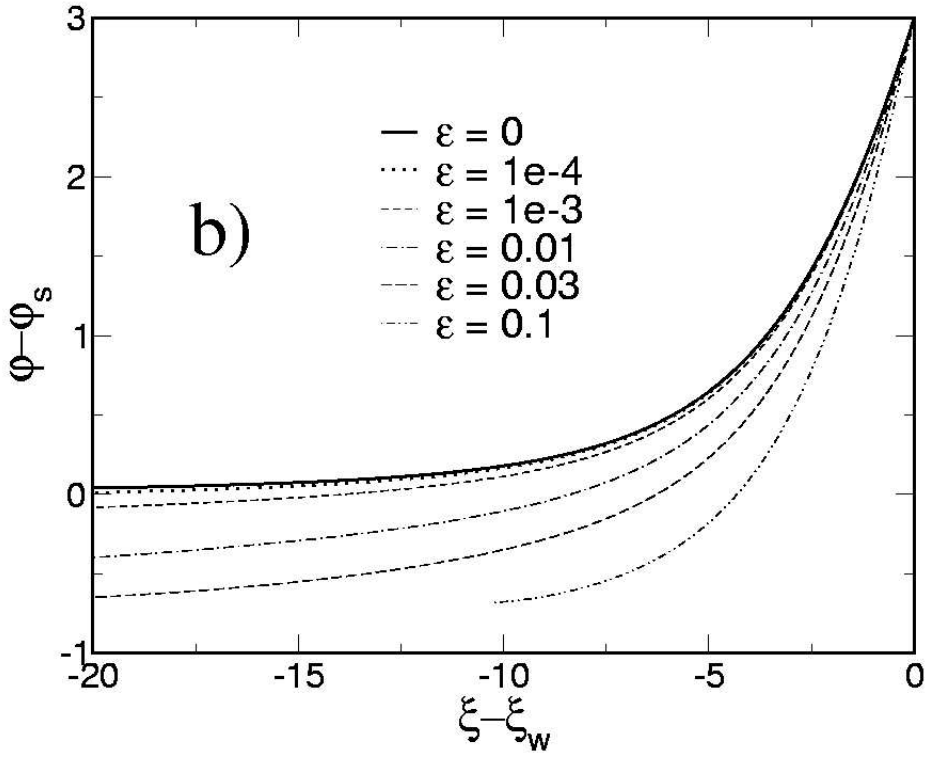

Figure 2: Normalized potential curves for the plane Tonks-Langmuir model with finite ϵ on the sheath scale.

In the asymptotic limit $\varepsilon \to 0$ the Poisson equation in set (4) collapses to the quasineutrality condition. The resulting set of equations, presented in (6) can be solved analytically. In this limit only the left boundary condition at the plasma center can be fullfilled and the solution for the potential runs into a singular point on the right, which is called the sheath edge. The set of equations from (4) is

$$\begin{aligned} \frac{d}{dx}(nu) &= e^{-\phi} \\ \frac{d}{dx}\left(\frac{u^2}{2} - \phi\right) &= -e^{-\phi}u/n \\ n &= e^{-\phi} \end{aligned} \tag{6}$$

A detailed derivation of the solution of the upper set of equations can be found in [4]. The solutions read

$$\begin{aligned} x &= 2\arctan(u) - u \\ \phi &= \ln(1+u^2) \\ n &= 1/(1+u^2) \end{aligned} \tag{7}$$

The sheath edge is defined as the point where $\phi = \phi_s = \ln 2$, $n = n_s = 1/2$, and $u =$ 1- the marginal Bohm criterion. Therefore $x_s = \pi/2 - 1$. At this point the electric field strength becomes infinity.,

$$\frac{d\phi}{dx} = \frac{2u}{1-u^2}. \tag{8}$$

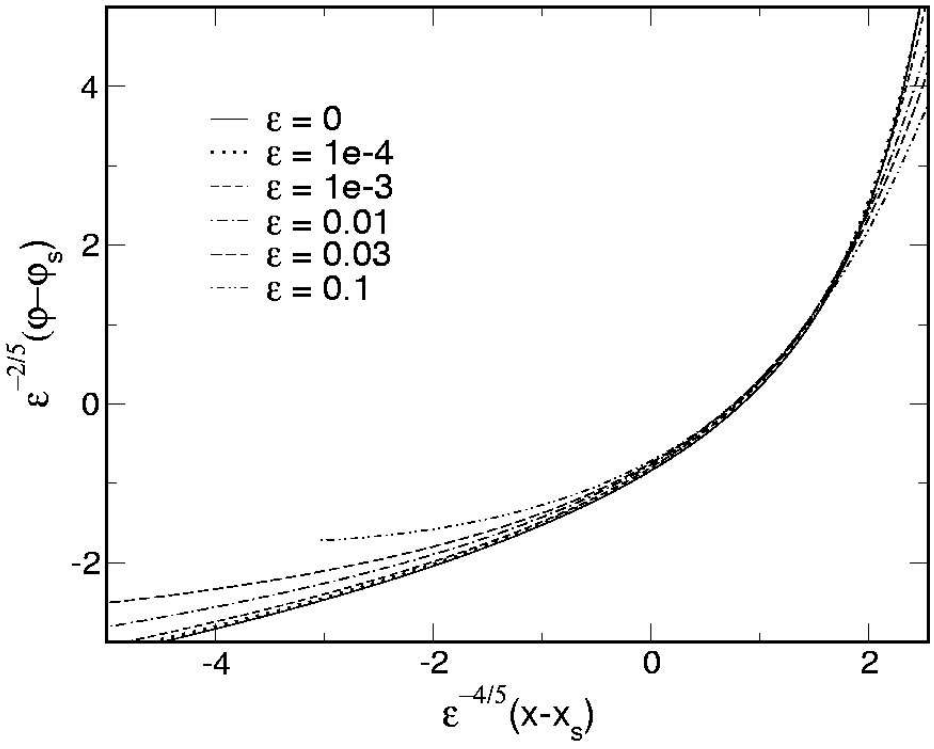

Figure 3: Normalized potential curves for the plane Tonks-Langmuir model with finite ϵ on the intermediate scale.

The solutions (7) are the first parts which are needed for the matching procedure. Approaching the sheath edge, $1 - u \ll 1$, the potential profile may be approximated by the parabola

$$\phi_{oi}(x) = \phi_s - \sqrt{2(x_s - x)}, \qquad x < x_s, \tag{9}$$

called the "inner expansion" of the presheath ("outer") solution.

3.2 Asymptotic Sheath Scale Analysis

In the sheath the Debye length λ_D is the characteristic scale, therefore it is natural to derive equations valid in the sheath with the normalization $\xi = (z - z_r)/\lambda_D$ (see Eqs. (5)). In the limit $\varepsilon \to 0$ one obtains the following set of equations

$$\begin{aligned} \frac{d}{d\xi}(nu) &= 0 \\ \frac{d}{d\xi}\left(\frac{u^2}{2} - \phi\right) &= 0 \\ \frac{d^2\phi}{d\xi^2} &= n - e^{-\phi} \end{aligned} \tag{10}$$

The solution is independent of the source/sink terms and is said to be universal, in a sense that it is valid for different problems. There cannot be found an analytical solution to the upper set of equations, but usually one can derive the so called sheath equation [13]

$$\frac{d^2\chi}{d\xi^2} = \frac{1}{2}\left(\frac{1}{\sqrt{1+2\chi}} - e^{-\chi}\right) \tag{11}$$

where the new variable $\chi = \phi - \ln 2$ was introduced. This equation is homogenuous in space that means that the solution can be shifted. Therefore the wall position cannot be determined from this equation. On the sheath scale the plasma is extended infinitely far away, that's why we can choose the potential $\chi \to 0$, the electric field $\left(\frac{d\chi}{d\xi}\right) \to 0$ and the ion velocity $u \to 1$ at $\xi \to -\infty$ as the boundary conditions for the sheath. From (11) for the electric field we find

$$\left(\frac{d\chi}{d\xi}\right)^2 = \sqrt{1+2\chi} + e^{-\chi} - 2 \tag{12}$$

We can generalize the boundary condition for the ion velocity choosing $u \to u_0$ at $\xi \to -\infty$. Then the straightforward calculations lead to the Bohm criterion for the ion velocity u_0 at the sheath entrance. Really, Eq. (12) we can replace by

$$\left(\frac{d\chi}{d\xi}\right)^2 = u_0^2\sqrt{1+2\chi/u_0^2} + e^{-\chi} - 1 - u_0^2. \tag{13}$$

Near the sheath entrance, where $\chi \ll 1$, we find

$$\left(\frac{d\chi}{d\xi}\right)^2 = \frac{1}{2}\left(1 - \frac{1}{u_0^2}\right)\chi^2, \tag{14}$$

and the positiveness of the left-hand side leads to the relation

$$u_0^2 \geqslant 1,$$

known as the Bohm criterion. In Eqs. (11) and (12) the Bohm criterion is used in the marginal form, $u_0 = 1$.

Expending Eq.(12) in the vicinity of the sheath edge, $\chi \ll 1$, we find the "outer" expamnsion of the sheath ("inner") solution

$$\chi(\xi) \to \chi_{io}(\xi) = \frac{12}{(\xi - \xi_0)^2}, \qquad \xi < \xi_0. \tag{15}$$

The solution (15) corresponds to the decaying sheath field. ξ_0 is an integration constant pointing to the fact that the sheath problem represented by Eqs.(10) (with boundary conditions $\left(\frac{d\chi}{d\xi}\right) \to 0$ at $\chi \to 0$) is homogeneous in space. Its numerical value depends, of course, on the choice of the origin of the space coordinate ξ (see the definition of ξ for Eqs. (5)).

3.3 Intermediate Scale Analysis

The main idea for an intermediate scale is to find a description of the problem in the transition region, where the quasineutrality condition, valid in the presheath, begins to be violated and in which also the ionization is to be taken into account. In other words in the transition region both the space charge and the ionization give small but finite contributions of the same order. We start from (4) and expand the source term in the continuity equation and the last term in the momentum equation into a Taylor series near the sheath edge. As in previous derivations of the presheath and the sheath approximations we are still doing the asymptotic theory, so in the limit $\varepsilon \to 0$ we know the position of the sheath edge and the values of our variables at the sheath edge. Near the sheath edge we can equate from (4) the following system

$$\begin{aligned} (nu)' &= 1/2 \\ uu' - \phi' &= -1 \end{aligned} \tag{16}$$

From these two equations one can easily find the ion density as a function of the potential. Expanding the resulting ion density n and the electron density $n_- = e^{-\phi}$ into a series one observes that the deviation of n and n_- arises in the second order in ϕ:

$$\begin{aligned} n &\approx 1/2(1 - \chi + 3/2\chi^2) + (x - x_s) \\ n_- &\approx 1/2(1 - \chi + 1/2\chi^2) \end{aligned} \tag{17}$$

where again $\chi = \phi - \ln 2$. Inserting (17) into Poisson equation leads to the following equation for the potential valid in the transition region

$$\epsilon^2 \frac{d^2\chi}{dx^2} = (1/2)\chi^2 + (x - x_s)$$

With a simple transformation $x = x_s + \epsilon^{4/5}\zeta$ and $\chi = \epsilon^{2/5} w$ we can derive a universal intermediate scale equation, which is independent of ε. Moreover it is universal in an extended sense, because it describes the plasma-sheath transition in any sheath problem in fluid analysis,

$$\frac{d^2 w}{d\zeta^2} = (1/2)w^2 + \zeta \tag{18}$$

This equation is known as Painleve equation of first kind and connot be solved analytically. Boundary conditions for large negative ζ can be found via an approach to the presheath region (left side from the sheath edge), where we expect quasineutrality and (18) collapses to $0 = 1/2w^2 + \zeta$. The corresponding solution,

$$w_l(\zeta) = -\sqrt{-2\zeta}, \tag{19}$$

is obviously identtical with the "inner" expansion (9) of the presheath solution. The approximation (19) can be used to determine the boundary conditions for the numerical integration. Differentiating (19) twice and inserting the result into (18) lead to

$$w^2 = 2(-2\zeta)^{-3/2} - 2\zeta, \tag{20}$$

$$w' = (6(-2\zeta)^{-5/2} - 2)/2w, \tag{21}$$

by which we improve the boundary conditions by one iteration step. A large negative value of ζ will give initial conditions for potential and its derivative, so that the Painleve equation can be integrated. One observes that the solution runs into a singularity at ζ_0, which lies in the domain of interest. From the numerical results we find $\zeta_0 = 3.918982$. Apart from the numerical difficulties this singularity will become very important later on in positioning the sheath solution. An approximation for w near ζ_0 (right side of the sheath edge) can be found if we neglect ζ in (18) and integrate

$$w_r(\zeta) = 12/(\zeta - \zeta_0)^2 \tag{22}$$

Obviously it corresponds to the "outer" expansion of the sheath solution (15). For $\varepsilon = \lambda_D/\lambda \to 0$ the whole transition region, $\zeta = O(1)$, $w = O(1)$, in the presheath scale is mapped into *one* pont $(z - z_s)/\lambda = (x - x_s) \sim \varepsilon^{-4/5}\zeta \to 0$, $\chi = (\phi - \phi_s) \sim \varepsilon^{2/5} w \to 0$: the *sheath edge.* The correspinding sheath limit $(z - z_s)/\lambda_D \sim \varepsilon^{-1/5}\zeta \to -\infty$, $\chi \to 0$ confirms the sheath boundary condition. The electric field in the transition region justifies the estimation

$$E \sim \frac{T_e \varepsilon^{2/5}}{e l_m} \sim \frac{T_e}{e \lambda_D^{2/5} \lambda^{3/5}} \tag{23}$$

Here the estimation $\chi \sim \varepsilon^{2/5}$ (at $w = O(1)$) for the potential in the transition region is used. This expression for the electric field elucidates the limits

$$\left|\frac{\partial \phi}{\partial \xi}\right| \sim \frac{e\lambda_D E}{T_e} \sim \varepsilon^{3/5} \to 0 \quad \text{and} \tag{24}$$

$$\left|\frac{\partial \phi}{\partial x}\right| \sim \frac{e\lambda E}{T_e} \sim \varepsilon^{-2/5} \to \infty \tag{25}$$

of the vanishing sheath edge field on the sheath scale and an infinite field on the presheath scale without any contradiction.

4. The Matching Problem

In Section 3 we have derived two solutions, one valid for the presheath region and the other valid for the sheath region. These two solutions can not be matched directly because they don't have a common range of validity, which is expressed by the matching condition, given in [18],[19]:

$$Y_{io} = Y_{oi}$$

In the special problem considered here one finds from Eqs.(7) the presheath solution close to the sheath edge (the inner expansion of the outer solution)

$$\phi_{oi}(x) - \phi_s = -\sqrt{-2(x - x_s)} \tag{26}$$

From Eq.(11) we can also make an expansion to find the sheath solution near the sheath edge ($\xi \to -\infty, \chi \to 0$)

$$\chi_{io}(\xi) = \phi_{io}(\xi) - \phi_s = \frac{12}{(\xi - \xi_0)^2}, \tag{27}$$

with an arbitrary integration constant ξ_0 accounting for the space homogenity of Eq.(11). Obviously the limiting expressions (27) and (26) are not identical and a direct smooth matching is not possible. Another problem arises because in the derivation of (27) the integration constant ξ_0 cannot be detemined in the frame of the sheath scale analysis.
On the other hand Eq.(22) is identical with the "outer" expansion of the the inner solution [see Eq. (27)] if we define $\xi_0 = \left\{x_s - x_r + \epsilon^{4/5}\zeta_0\right\}\varepsilon^{-1}$. The position of χ_{io} can now be fixed with ζ_0 and further the position of the sheath solution of equation (11) can also be determined.
Similarily we find that Eq.(19) represents Eq.(26) on the intermediate scale. From that we see that the intermediate scale ζ is necessary to bridge the gap between the plasma and the sheath solution. The matching procedure for the full problem consists of two parts, namely matching the plamsa solution with the intermediate solution and the intermediate solution with the sheath solution. For this problem two matching conditions have to be fulfilled:

$$\phi_{oi}(x) - \phi_s = \varepsilon^{2/5} w_l(\zeta) = \varepsilon^{2/5} w_l(\varepsilon^{-4/5}(x - x_s)), \tag{28}$$

$$\phi_{io}(\xi) - \phi_s = \phi_{io}(x/\epsilon) - \phi_s = \varepsilon^{2/5} w_r(\zeta) = \tag{29}$$

$$= \varepsilon^{2/5} w_r(\varepsilon^{-4/5}(x - x_s)).$$

As it is mentioned above the second condition is fullfiled if we set $\xi_0 = \left\{x_s - x_r + \epsilon^{4/5}\zeta_0\right\}\varepsilon^{-1}$. Now we can find the matched solution with the formula

$$\phi(x) = \phi_o(x) - \phi_{oi}(x) + \varepsilon^{2/5} w(\varepsilon^{-4/5}(x - x_s)) - \phi_{io}(x/\varepsilon) + \phi_i(x/\varepsilon), \tag{30}$$

which was given in [12],[7], but was never evaluated. In Fig.4 all parts needed to evaluate (30) are shown on the presheath scale. The smallness parameter was chosen $\epsilon = 0.01$.

The presheath solution and its approximate solution (the parabola (26)) exist only for $x - x_s \leqslant 0$ and must be defined as equal to zero, $\phi_o(x) - \phi_{oi}(x) = 0$, for $x > x_s$. Similarly the intermediate solution $w(\zeta)$ and its asymptote $w_r(\zeta)$ exist only for $\zeta \leqslant \zeta_0$. In the numerical procedure the singularities lead to severe problems because of the necessity that the differences $\phi_o(x) - \phi_{oi}(x)$ and $\epsilon^{2/5} w(\epsilon^{-4/5}(x - x_s)) - \phi_{io}(x/\epsilon)$ must tend to zero at $x \to x_s$ and $\zeta \to \zeta_0$ respectively. To achieve good results analytic continuations have to be used at these special points. The amazing results are shown in Fig.5. One can see that even for big values of ε a smooth matching is possible.

5. The Eigenvalue problem

We have already said that the wall position x_w is not a priori given, but is an eigenvalue of the problem. This eigenvalue is calculated by cutting the solution at that position $x = x_w$ fullfilling

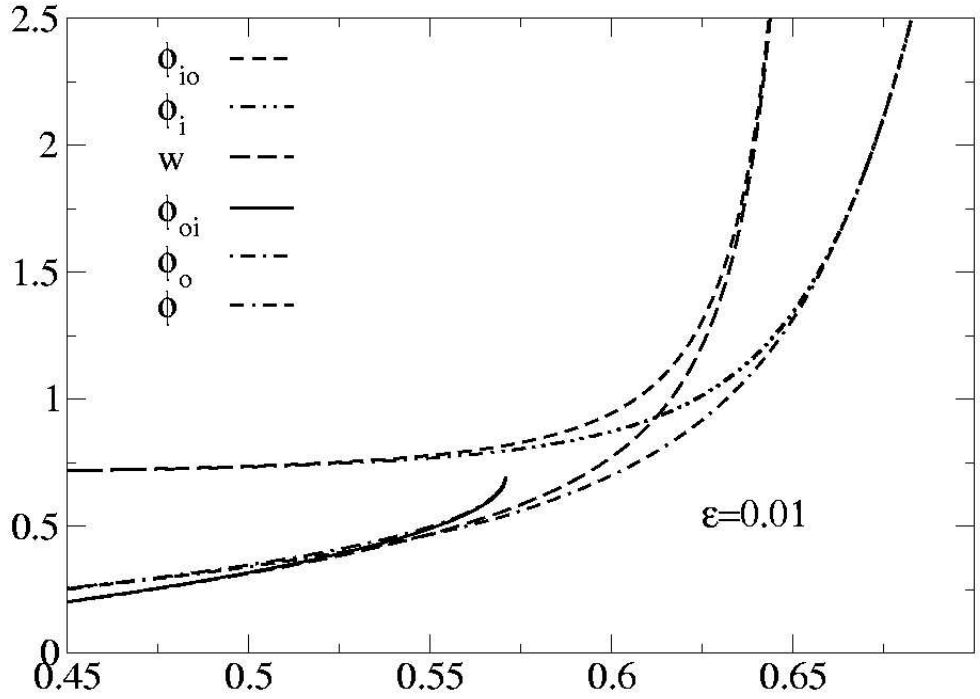

Figure 4: Normalized potential curves in the vicinity of the sheath edge, outer expansion of the sheath solution ϕ_{io}, sheath solution ϕ_i, intermediate solution w, inner expansion of the presheath solution ϕ_{oi}, presheath solution ϕ_o and the curve corresponding to the matched solution ϕ from Eq. (30).

the wall boundary condition $\phi = \phi_w$. We formulate the boundary condition by prescribing the wall potential ϕ_w and write formally

$$x_w = L(\phi_w, \varepsilon). \tag{31}$$

Our numerical evaluations refer to a wall potential $\phi_w = 5.375$ corresponding to the floating potential in Argon [11]. The exact eigenvalue $L(5.375, \epsilon) = L(\varepsilon)$ obtained by numerical integration of Eqs.(4) are listed in Table (second column).

ε	$L(\varepsilon)$	$L_1(\varepsilon)$	$L_2(\varepsilon)$
0	0.570796	0.570796	0.570796
1e-5	0.57123	0.571236	0.571230
3e-5	0.57186	0.571884	0.571859
1e-4	0.57365	0.573749	0.573643
3e-4	0.57780	0.578191	0.5777894
1e-3	0.57952	0.571199	0.579516
3e-3	0.57640	0.572770	0.576481
1e-2	0.57981	0.577242	0.570568

Table1: Eigenvalue $L(\varepsilon)$ and approximations $L_1(\varepsilon)$ and $L_2(\varepsilon)$ [see Eq. (32) and Eq. (33)]

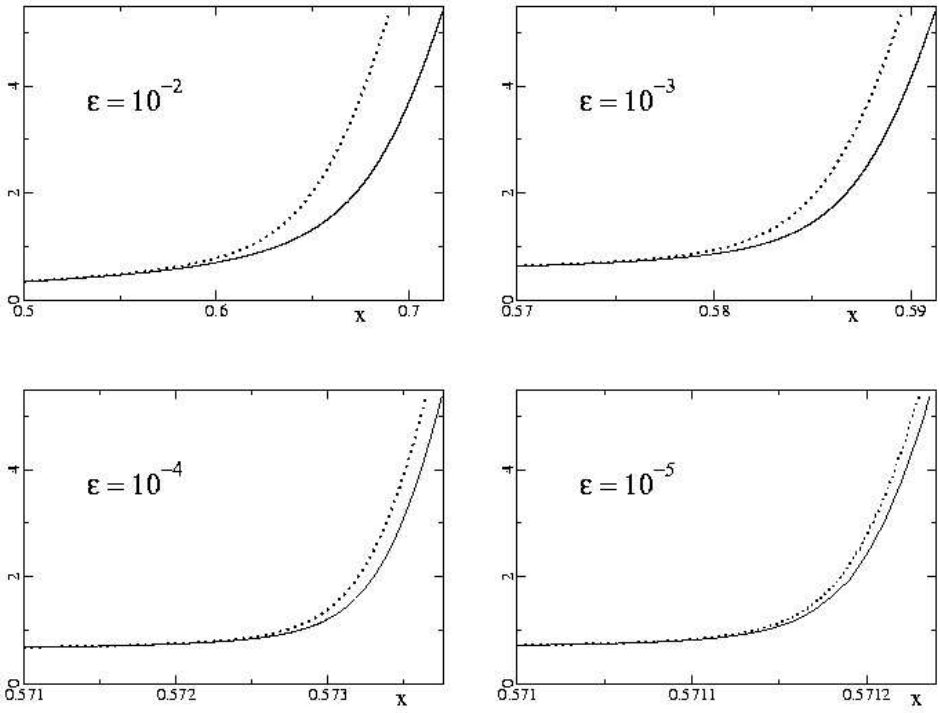

Figure 5: Matched solution (30) (solid line) and numerical solution of the system (4) (dotted line) for the potential $\phi(x)$ on the presheath scale x.

Physically the eigenvalue represents the ionization rate necessary to fulfill the plasma balance. The asymptotic analysis presented in the preceding sections gives us a tool to construct approximate eigenvalues. In zero order, $\varepsilon \to 0$, , we obtain

$$L_0 = x_s = \frac{\pi}{2} - 1,$$

i.e., the position of the wall and the sheath edge are identical. However we may obtain a better approximation for small but finite ε if we account for the finite extension of the intermediate scale and the sheath:

1. The presheath extension (measured from the center to the sheath edge) is given by $L_0 \equiv x_s$.
2. The extension of the intermediate scale (measured from the sheath edge to the intermediate singularity) is given by $\varepsilon^{4/5}\zeta_0$.
3. The extension of the sheath (measured from the intermediate singularity to the wall) is given by $(\xi_w - \xi_0)\varepsilon$.

Summarizing these contributions we obtain the approximation

$$L_1 = \frac{\pi}{2} - 1 + \varepsilon^{4/5}\zeta_0 + (\xi_w - \xi_0)\varepsilon. \tag{32}$$

The sheath extension $(\xi_w - \xi_0)$ is obtained by cutting the sheath solution at the point where the wall boundary condition is fullfilled. It depends on the wall potential ϕ_w but not on ε. The approximation $L_1(5.375, \varepsilon) \equiv L_1(\varepsilon)$ is listed in the third column of Table. Obviously the eigenvalue (i.e, the system extension) is overestimated for finite ε. This is in agreement with the results shown in Fig.5, which suggest that the sheath solution must be shifted to the left to obtain a better fitting.
Eq (32) appears to be the begin of a Taylor series in the scale ratio $\varepsilon^{1/5}$ of the sheath and intermediate scales. This supposition is supported by the numerical results because the error increases approximately with $\varepsilon^{6/5}$. This means that we can improve L_1 and expect better approximation by setting

$$L_2 = \frac{\pi}{2} - 1 + \zeta_0\varepsilon^{4/5} + (\xi_w - \xi_0)\varepsilon + a\varepsilon^{6/5}. \tag{33}$$

This expectation is confirmed by the numerical results. In Table we have listed $L_2(5.375, \varepsilon) \equiv L_2(\varepsilon)$ with $a \approx -6.6$. A more accurate determination of a from the numerical results is difficult because we have to choose ε so small that $\varepsilon^{7/5}$ can be neglected in comparison to $\varepsilon^{6/5}$. On the other hand, for such small ε the correction $a\varepsilon^{6/5}$ is hardly significant.

PWT layer without its splitting

In this section we consider a PWT layer wich is one-dimensional in space along the z direction. The bounding wall surface is assumed to be a plane perpendicular to the z axis and is placed at $z = 0$, see Fig.6. It is negatively charged and all particles impinging on it are absorbed. The plasma occupies the region $z < 0$.

6. General theory

The electrostatic potential φ is governed by Poisson's equation,

$$-\frac{\partial^2}{\partial z^2}\varphi(z) = 4\pi \sum_\alpha e_\alpha n_\alpha(z), \tag{34}$$

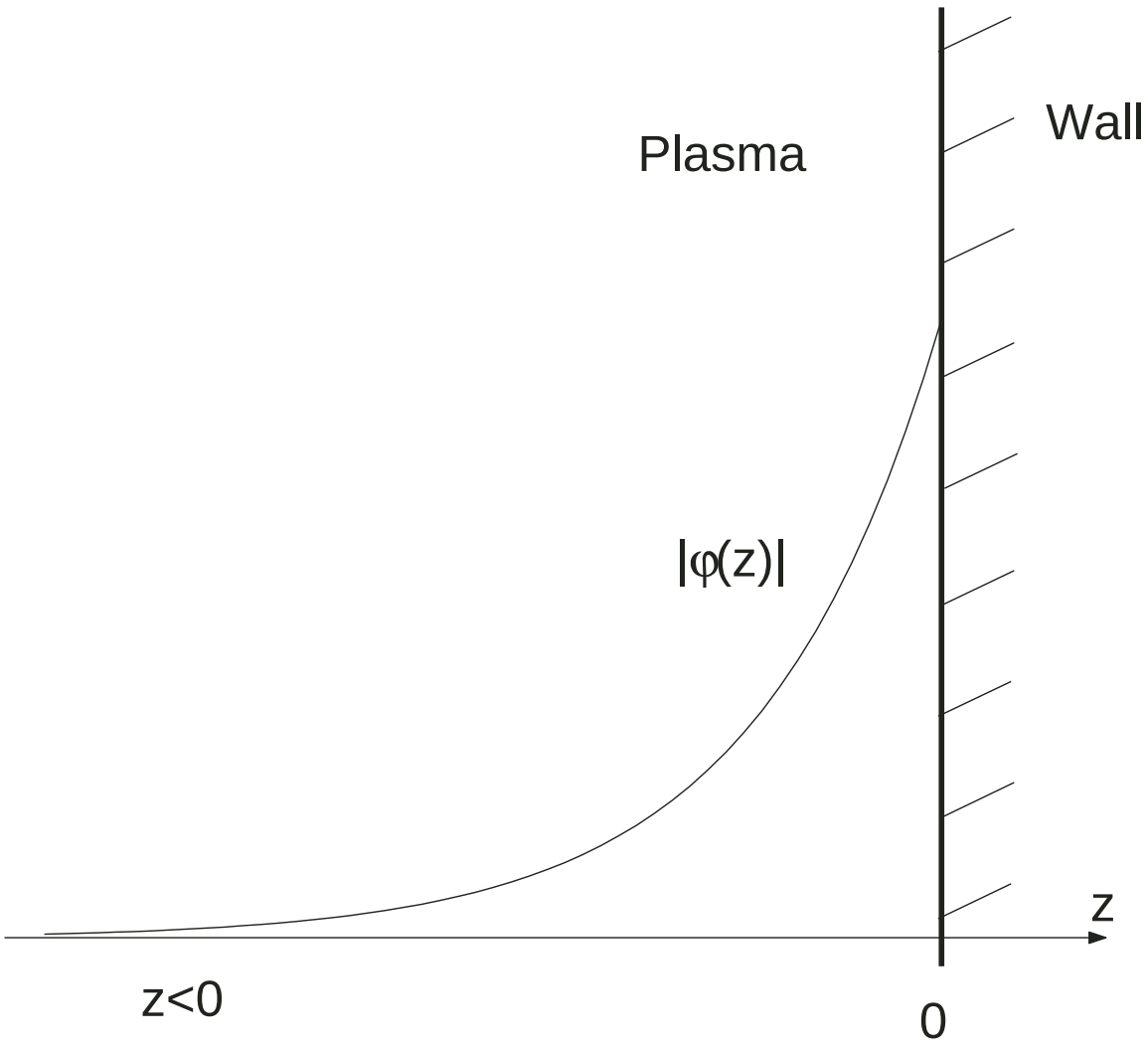

Figure 6: The geometry of the plasma-wall transition (PWT)

where n_α and e_α are the density and the electric charge of particle species α, respectively; the subscript α equals e for electrons and i for ions. The electron and ion charges are $e_e = -e$, $(e > 0)$ and $e_i = e$, respectively. The dynamics of the plasma particles is governed by the Boltzmann (kinetic) equation,

$$v_z \frac{\partial f_\alpha}{\partial z} - \frac{e_\alpha}{m_\alpha} \frac{\partial \varphi}{\partial z} \frac{\partial f_\alpha}{\partial v_z} = \sum_\beta C_{\alpha\beta} \{f_\alpha; f_\beta\}, \tag{35}$$

where f_α and f_β are the distribution functions of particle species α and β, respectively, $C_{\alpha\beta}\{f_\alpha, f_\beta\}$ is the collision integral for collisions between species α and β, β equals e and i for the charged particles and n for the neutrals, and m_α is the mass of a species-α particle. The sum in Eq. (34) is taken over the charged particles only ($\alpha = e, i$), while the one in Eq. (35) also includes neutrals ($\beta = e, i, n$).

The density of particle species α is obtained by integrating the species-α particle distribution function as

$$n_\alpha = \int f_\alpha(z, \mathbf{v}) d\mathbf{v}. \tag{36}$$

Multiplying Eq. (34) by $\partial\varphi(z)/\partial z$, we obtain

$$-\frac{1}{2}\frac{\partial}{\partial z}\left[\frac{\partial \varphi(z)}{\partial z}\right]^2 = 4\pi \sum_\alpha e_\alpha n_\alpha \frac{\partial \varphi(z)}{\partial z}. \tag{37}$$

From the kinetic equation (35) it follows that

$$e_\alpha n_\alpha \frac{\partial \varphi(z)}{\partial z} = -\frac{\partial}{\partial z}\int m_\alpha v_z^2 f_\alpha d\mathbf{v} + \sum_\beta m_\alpha \int v_z C_{\alpha\beta}\left\{f_\alpha; f_\beta\right\} d\mathbf{v}, \tag{38}$$

which we insert into Eq. (37) to obtain

$$\frac{\partial}{\partial z}\left\{-\frac{1}{8\pi}\left[\frac{\partial \varphi(z)}{\partial z}\right]^2 + \sum_\alpha \int m_\alpha v_z^2 f_\alpha d\mathbf{v}\right\} = \sum_{\alpha\beta} m_\alpha \int v_z C_{\alpha\beta}\left\{f_\alpha; f_\beta\right\} d\mathbf{v}, \tag{39}$$

where the term on the right-hand side of Eq. (39) describes the momentum gain (or loss) by α-particles due to collisions with β-particles.

According to standard gas kinetic theory we have [20]

$$\int m_\alpha v_z^2 f_\alpha d\mathbf{v} = m_\alpha n_\alpha(z) u_\alpha^2(z) + n_\alpha(z) T_\alpha(z), \tag{40}$$

where the fluid velocity $u_\alpha(z)$ and the temperature $T_\alpha(z)$ of the gas of α-particles are defined by

$$n_\alpha(z) u_\alpha(z) = \int v_z f_\alpha d\mathbf{v}, \tag{41}$$

and

$$n_\alpha(z) T_\alpha(z) = \int m_\alpha [v_z - u_\alpha(z)]^2 f_\alpha d\mathbf{v}. \tag{42}$$

Inserting Eqs. (40) and (41) into Eq. (39), we obtain

$$\frac{\partial}{\partial z}\left\{-\frac{1}{8\pi}\left[\frac{\partial \varphi(z)}{\partial z}\right]^2 + \sum_\alpha \left[m_\alpha n_\alpha(z) u_\alpha^2(z) + n_\alpha(z) T_\alpha(z)\right]\right\} = \sum_{\alpha\beta} m_\alpha \int v_z C_{\alpha\beta}\left\{f_\alpha; f_\beta\right\} d\mathbf{v}. \tag{43}$$

We now estimate the contributions of the following collision processes:

- Elastic and ionization collisions of electrons with neutrals.
- Elastic and charge-exchange collisions of ions with neutrals, and increase of the ion number density due to the ionization collisions of electrons with neutrals.
- Recombination of ions with electrons, which far away from the boundary (i.e., at distances $\gtrsim l_{ps}$) balances the ionization processes.

According to the momentum conservation law, the elastic collision integrals satisfy the relations [20]

$$\int v_z C_{\alpha\alpha}^{el}\left\{f_\alpha; f_\alpha\right\} d\ \mathbf{v} = 0, \tag{44}$$

and

$$m_\alpha \int v_z C_{\alpha\alpha'}^{el}\left\{f_\alpha; f_{\alpha'}\right\} d\mathbf{v} + m_{\alpha'} \int v_z C_{\alpha'\alpha}^{el}\left\{f_{\alpha'}; f_\alpha\right\} d\mathbf{v} = 0 \quad \text{where} \quad \alpha \neq \alpha'. \tag{45}$$

Therefore, in the summation over β on the right-hand side of Eq. (39), the only terms remaining for the elastic collisions are the terms with $\beta = n$. Thus,

$$\sum_{\alpha\beta} m_\alpha \int v_z C_{\alpha\beta}^{el}\left\{f_\alpha; f_\beta\right\} d\mathbf{v} = \sum_\alpha m_\alpha \int v_z C_{\alpha n}^{el}\left\{f_\alpha; f_n\right\} d\mathbf{v}, \tag{46}$$

which describes the momentum loss by charged particles due to elastic collisions with neutrals. The sum on the right-hand side of Eq. (43) can now be written in the form

$$\sum_{\alpha\beta} m_\alpha \int v_z C_{\alpha\beta}\left\{f_\alpha, f_\beta\right\} d\mathbf{v} =$$
$$\int d\mathbf{v} v_z \left[m_e\left(C_{en}^{el}\left\{f_e; f_n\right\} + C_{en}^{ion}\left\{f_e; f_n\right\} + C_{ei}^{rec}\left\{f_e; f_i\right\}\right) +\right.$$
$$\left. m_i\left(C_{in}^{el}\left\{f_i; f_n\right\} + C_{in}^{cx}\left\{f_i; f_n\right\} + C_{in}^{ion}\left\{f_e; f_n\right\} + C_{ie}^{rec}\left\{f_i; f_e\right\}\right)\right], \tag{47}$$

where we have assumed $m_i \simeq m_n$.

In what follows, we shall make the following assumptions enabling us to proceed analytically.

1. The number densities of the electrons and ions are much less than the number density of the neutrals, viz. $n_e, n_i \ll n_n$. The neutrals are assumed to be cold without drift velocity so that $f_n = n_n\delta(v)$, with the Dirac δ-function $\delta(v)$. In the weakly ionized plasma the number density of the energetic neutrals, generated by charge-exchange collisions with the accelerated ions, is small and hence can be neglected

2. In elastic electron-heavy neutral particle collisions, due to the extremely different masses of scattering partners, the velocity vector of electrons is changed in angle but (almost) not in magnitude. If elastic collisions are frequent and the electric field is not too high, the drift velocity of electrons proves to be small compared to the chaotic thermal velocity. This implies that the electron distribution is mostly spherical and isotropic in the velocity space. Therefore the elastic and ionization collisions of electrons with neutrals we can describe in the so-called "two term approximation" [21], and consider only the zeroth-order collision terms [22, 23]. In this approximation, the electron collision term $C_{en}^{el}\left\{f_e; f_n\right\}$ and $C_{en}^{ion}\left\{f_e; f_n\right\}$ are isotropic in the velocity space and the corresponding terms in Eq. (47) vanish.

   It should be also mentioned that due to the extremely different masses of eletron and neutral particle, the therm of electron-neutral elastic collision term is negligible for most discharges where the typical electron energy is of order of some eV.

3. The ionization process is realized by the electron-neutral collisions. We represent ionization collision term $C_{in}^{ion}\left\{f_e; f_n\right\}$ in the ion kinetic equation in a form which is commonly used in the plasma sheath problem [15], [14, 16, 24],.

$$C_{in}^{ion}\left\{f_e; f_n\right\} = \nu_{ion} n_e(z)\delta(\mathbf{v}), \tag{48}$$

   where ν_{ion} is the frequency of electron-neutral ionization collisions. The appearance of the δ-function in (48) is due to the distribution function of neutrals. This collision term satisfies the equality:

$$\int d\mathbf{v}\, m_i v_z C_{in}^{ion}\left\{f_e; f_n\right\} = 0. \tag{49}$$

4. For the recombination collision terms $C_{ei}^{rec}\left\{f_e; f_i\right\}$ and $C_{ie}^{rec}\left\{f_i; f_e\right\}$ we use the simple models [15],

$$C_{ei}^{rec}\left\{f_e; f_i\right\} = -\gamma n_i(z) f_e, \tag{50}$$
$$C_{ie}^{rec}\left\{f_i; f_e\right\} = -\gamma n_e(z) f_i, \tag{51}$$

   where γ is the constant recombination coefficient. Due to $m_i \gg m_e$ (see the coefficients at $C_{ei}^{rec}\left\{f_e; f_i\right\}$ and $C_{ie}^{rec}\left\{f_i; f_e\right\}$ in the right-hand side of (47)) the friction force connecterd with $C_{ei}^{rec}\left\{f_e; f_i\right\}$ is much smaller than the force with $C_{ie}^{rec}\left\{f_i; f_e\right\}$.

5. The cross-section of ion-neutral charge-exchange collisions is much larger than the cross-section of ion-neutral elastic scattering [16, 25, 26], viz.

$$\sigma_{in}^{cx} \gg \sigma_{in}^{el}, \tag{52}$$

which leads to

$$R_{in}^{cx} \gg R_{in}^{el}. \tag{53}$$

where the friction force acting on the ions due to their charge-exchange collisions with neutrals and the force connected with the ion-neutral elastic collisions are defined as

$$R_{in}^{cx} = \int d\mathbf{v}\, m_i v_z C_{in}^{cx} \{f_i; f_n\}, \tag{54}$$

and

$$R_{in}^{el} = \int dv\, m_i v_z C_{in}^{el} \{f_i; f_n\}.$$

Similarly we define the friction force acting on ions due to the recombination,

$$R_{ie}^{rec} = \int d\mathbf{v}\, m_i v_z C_{ie}^{rec} \{f_i; f_e\}. \tag{55}$$

According to the above assumptions and Eq. (47), we obtain from Eq. (43)

$$\frac{\partial}{\partial z}\left\{-\frac{1}{8\pi}\left[\frac{\partial \varphi(z)}{\partial z}\right]^2 + \sum_\alpha \left[m_\alpha n_\alpha(z) u_\alpha^2(z) + n_\alpha(z) T_\alpha(z)\right]\right\} = \tag{56}$$

$$= R_i = R_{in}^{cx} + R_{ie}^{rec}.$$

We note that $R_{in}^{cx} < 0$, $R_{ie}^{rec} < 0$ and $R_i < 0$. According to Refs.[16, 27, 28], we have

$$C_{in}^{cx} = \int d\mathbf{v}_n \left[f_n(\mathbf{v}) f_i(z, \mathbf{v}_n) - f_n(\mathbf{v}_n) f_i(z, \mathbf{v})\right] |\mathbf{v} - \mathbf{v}_n|\, \sigma_{in}^{cx}(|\mathbf{v} - \mathbf{v}_n|). \tag{57}$$

For the cold neutrals assumed we find

$$R_{in}^{cx}(z) = -\int d\mathbf{v} m_i v_z \frac{|\mathbf{v}|}{\lambda_{cx}(|\mathbf{v}|)} f_i(z, \mathbf{v}), \tag{58}$$

where

$$\lambda_{cx} = (n_n \sigma_{in}^{cx} |\mathbf{v}|)^{-1} \tag{59}$$

is the ion mean free path associated with charge-exchange collisions. The recombination collision term, modeled in the form (51), leads to the following loss of ion momentum

$$R_{ie}^{rec} = -\gamma n_e(z) \int d\mathbf{v}\, m_i v_z f_i(z, \mathbf{v}), \tag{60}$$

This model corresponds to the recombination frequency $\nu_{rec}(z) = \gamma n_e(z)$.

The relation (56) represents the balance of the electric field pressure force, the total particle momentum flux, the gas kinetic pressure force, and the ion friction force.

Far away from the boundary ($z \to -\infty$), the uniform ($\partial/\partial z = 0$) plasma is characterized by the quasi-neutrality condition, i. e., $n_e = n_i = n_0$, and by a balance between the ionization and recombination of charged particles. In fact, the recombination we have introduced here in order to avoid the accumulation of an infinite density of charged particles starting to move from large distances towards the wall.

Note that, although the friction force connected with ionization does not appear explicitly in Eq. (56), we have to account for the ionization collisions in the ion kinetic equation in order to calculate correctly the ion density and velocity.

Equation (56) is valid for any spatial point. It embraces both the presheath and sheath regions of the plasma-wall transition layer and thus allows us to describe the layer without the necessity of splitting it into these two regions.

8. The generalized Bohm criterion for a semi-bounded plasma

From the balance relation (56) we will now derive a generalized Bohm criterion. Let us consider a semi-bounded plasma (see Fig.6), when the plasma extends to $z \to -\infty$ with the natural boundary conditions $\varphi(z) \to 0$, $(\partial\varphi(z)/\partial z) \to 0$, $n_e(z) \to n_{e0}$, $n_i(z) \to n_{i0}(= n_{e0} = n_0)$ and $u_i(z) \to 0$. For the cold ions we neglect the ion thermal motion, $T_i \to 0$. We also neglect the fluid velocity of electrons in comparison with their thermal velocity, $m_e u_e^2 \ll T_e$. After integrating Eq. (56) over the interval $(-\infty, z)$, the nonnegativeness of $(\partial\varphi(z)/\partial z)^2$ implies the inequality

$$u_i^2(z) \geq \frac{n_0}{n_i(z)} c_{s0}^2 \left[1 - \frac{n_e(z)}{n_0} - \frac{1}{n_0 T_{e0}} \int_{-\infty}^{z} dz' \left| R_i(z') \right| \right], \tag{61}$$

where $c_{s0}(= \sqrt{T_{e0}/m_i})$ is the ion sound speed, T_{e0} is the electron temperature at $z \to -\infty$, and $R_i(z)$ is defined in Eq. (56). In obtaining Eq. (61) we have assumed that the electron temperature changes only slightly throughout the transition layer, and therefore we neglect its change and take $T_e(z) = T_{e0}$.

Equation (61) has the form of a generalized Bohm criterion. As in the Introduction, it is termed "non-marginal" or "marginal", depending on whether the inequality or the equality sign applies, respectively. We emphasize that, since it follows from Eq. (56), the generalized Bohm criterion must be fulfilled in its non-marginal form at any finite z inside the PWT layer, and tends to its marginal form only for $z \to -\infty$, where $u_i(z) \to 0$. Note that it has been obtained without splitting the PWT layer into separate sheath and presheath regions [14, 16]. In other words, we apply Poisson's equation everywhere, rather than replacing it with the quasineutrality condition in the presheath region. From Eq. (61) it follows that the friction force decreases the threshold value of the ion fluid velocity in the Bohm criterion.

Obviously, in the appropriate limit the generalized Bohm criterion (61) has to yield the original form of the Bohm criterion. This can be shown following the procedure described in Refs. [16, 26, 5]. In Refs. [16, 5], the spatial scales for the presheath and sheath are assumed to satisfy $\varepsilon \equiv \lambda_{Ds}/l_{ps} \to 0$ (asymptotic two-scale approximation, cf.the Introduction), and the sheath is considered to be collisionless, so that $R_i \simeq 0$. The potential and the electric field at the sheath edge are zero, the ions are assumed to be cold and, the electron fluid velocity is neglected. Integrating Eq.(56) over the interval (z_s, z), where z_s denotes the position of the sheath edge, we obtain

$$\frac{1}{8\pi} \left[\frac{\partial\varphi(z)}{\partial z} \right]^2 = m_i n_{is} u_{is} \left[u_i(z) - u_{is} \right] + n_e(z) T_e(z) - n_{es} T_{es}, \tag{62}$$

where $n_{\alpha s}$, u_{is} and T_{es} are the density, the fluid velocity and the temperature, respectively, of the particle species $\alpha(= e, i)$ at the sheath edge. In (62), we have used the continuity equation

$$n_i(z) u_i(z) = n_{is} u_{is} \tag{63}$$

for the ions. From the equation of motion, the ion velocity is obtained as

$$u_i(z) = \left[u_{is}^2 - \frac{2e}{m_i} \varphi(z) \right]^{\frac{1}{2}}. \tag{64}$$

The electron temperature is assumed to be unchanged throughout the sheath, viz. $T_e(z) = T_{es}$. For the electron density we choose the Boltzmann distribution (68) with $n_0 = n_{es}$.

Substituting Eq.(64) and the electron density into Eq.(62) and expanding the right-hand side in a Taylor series of powers of small $|\varphi(z)|$ we obtain the condition (Bohm criterion) for the existence of non-oscillatory solutions in the usual form

$$u_{is}^2 \geqslant c_s^2, \tag{65}$$

where $c_s = (T_{es}/m_i)^{\frac{1}{2}}$ is the ion sound speed at the sheath edge.

9. The potential profile in the semi-bounded plasma

The electron thermal speed is much larger than the ion speed, $V_{Te} \gg < v >_i$, where $< v >_i$ is the ion averaged speed. Further we are interested in the case when

$$\frac{< v >_i}{l_{ps}} \approx \nu_{cx},\ \nu_{ion},\ \nu_{rec}, \tag{66}$$

where l_{ps} is the characteristic presheath scale introduced above. Consequently we have

$$\frac{V_{Te}}{l_{ps}} \gg \nu_{ion}, \nu_{rec}, \tag{67}$$

and in the electron kinetic equation the ionization and recombination collisions can be neglected. The inequality (67) means that the number of electrons being newly born (due to ionization) or disappearing (due to recombination) during the time interval necessary for electrons to pass the distance l_{ps} is negligibly small. By contrast, according to Eq. (66) the time interval for ions to pass the distance l_{ps} is much larger and the number of newly generated and annihilated ions can be considerable.

In the special case considered below, we will assume the electron density to follow the Boltzmann distribution

$$n_e = n_0 \exp\left\{e\varphi(z)/T_e\right\}, \tag{68}$$

where n_0 is the electron density for $\varphi = 0$

We again consider, as in Sec.8, a semi-bounded plasma containing electrons, ions and neutrals, with a negatively charged wall at $z = 0$. For the ions we must solve the kinetic equation

$$v_z \frac{\partial f_i}{\partial z} + \frac{e}{m_i} \frac{\partial |\varphi(z)|}{\partial z} \frac{\partial f_i}{\partial v_z} = \left(\frac{\partial f_i}{\partial t}\right)_{cx} + \nu_{ion} n_e(z) \delta(v_z) - \gamma n_e(z) f_i, \tag{69}$$

taking onto account ionization, recombination and charge-exchange collisions. By means of $f_i(z, v_z)$, to be found from Eq. (69), we will calculate the ion density $n_i(z)$, the ion fluid velocity $u_i(z)$, and the friction force $R_{in}^{cx}(z)$ according to Eqs. (36), (41) and (58). Inserting the $n_i(z)$ thus found and the $n_e(z)$ following from Eq. (68) into Eq. (34) and solving the latter, we will find the potential profile.

As is well known, the charge-exchange collisions can be described, to a good approximation, by a constant cross section [14, 25]. Therefore, we assume that the mean free path for charge-exchange collision is constant, viz. $\lambda_{cx} = \text{const}$. Then we obtain from Eq. (58)

$$R_{in}^{cx}(z) = -\frac{1}{\lambda_{cx}} \int_0^\infty dv_z m_i v_z^2 f_i(z, v_z), \tag{70}$$

and the charge-exchange collision integral (57) takes the form

$$\left(\frac{\partial f_i}{\partial t}\right)_{cx} = C_{in}^{cx} = \frac{1}{\lambda_{cx}} \delta(v_z) \int_0^\infty v_z' f_i(z, v_z') dv_z' - \frac{v_z}{\lambda_{cx}} f_i(z, v_z). \tag{71}$$

Far away from the wall ($z \to -\infty$), where we assume the plasma to be quasineutral and uniform, we have $\varphi \to 0$, $\partial\varphi/\partial z \to 0$, $\partial f_i/\partial z \to 0$, and the left-hand side of Eq. (69) must vanish. For the distribution function we choose the boundary condition

$$f_i\left(z \to -\infty, v_z\right) = n_0 \delta(v_z). \tag{72}$$

In this asymptotic region, the ionization and recombination processes balance each other and the recombination coefficient is given by

$$\gamma = \frac{\nu_{ion}}{n_0}. \tag{73}$$

In what follows, the recombination coefficient γ will be replaced by the right-hand side of Eq. (73) and hence will not show up explicitly any more. In these conditions, the solution of Eq. (69) reads

$$\begin{aligned} f_i \;=\; & n_0 \frac{1}{v_z} \sqrt{v_z^2 + \frac{2e}{m_i}\varphi(z)}\, \delta\left(v_z - \sqrt{-\frac{2e}{m_i}\varphi(z)}\right) \times \\ & \times \exp\left(-\int_{z_0}^{z} dz' \left\{ \frac{1}{\lambda_{cx}} + \frac{\nu_{ion}}{n_0} \frac{n_e(z')}{\sqrt{v_z^2 - \frac{2e}{m_i}\left[\varphi(z') - \varphi(z)\right]}} \right\}\right) + \\ & + \int_{z_0}^{z} dz' S(z') \frac{1}{v_z} \delta\left(v_z - \sqrt{\frac{2e}{m_i}\left[\varphi(z') - \varphi(z)\right]}\right) \times \\ & \times \exp\left(-\int_{z'}^{z} dz'' \left\{ \frac{1}{\lambda_{cx}} + \frac{\nu_{ion}}{n_0} \frac{n_e(z'')}{\sqrt{v_z^2 - \frac{2e}{m_i}\left[\varphi(z'') - \varphi(z)\right]}} \right\}\right), \\ \text{for} \quad z_0 \;\to\; & -\infty, \end{aligned} \tag{74}$$

where

$$S(z) = \frac{1}{\lambda_{cx}} J_i(z) + \nu_{ion} n_e(z). \tag{75}$$

Note that there are no ions with $v_z < 0$. The ion flux $J_i(z)$ equals

$$\begin{aligned} J_i(z) \;\equiv\; & \int_0^{\infty} dv_z v_z f_i(z, v_z) = \int_{z_0}^{z} dz' \left(\frac{1}{\lambda_{cx}} J_i(z') + \nu_{ion} n_e(z')\right) \\ & \times \exp\left(-\int_{z'}^{z} dz'' \left\{ \frac{1}{\lambda_{cx}} + \frac{\nu_{ion}}{n_0} \frac{n_e(z'')}{\sqrt{v_z^2 - \frac{2e}{m_i}\left[\varphi(z') - \varphi(z'')\right]}} \right\}\right), \end{aligned} \tag{76}$$

where we have assumed that the ion flux vanishes at the point $z_0 \to -\infty$. For the ion density we have

$$\begin{aligned} n_i(z) \;\equiv\; & \int_0^{\infty} f_i(z, v_z) dv_z = n_0 \Delta(|\varphi(z)|) + \int_{z_0}^{z} dz' \frac{S(z')}{\sqrt{\frac{2e}{m_i}\left[\varphi(z') - \varphi(z)\right]}} \\ & \times \exp\left(-\int_{z'}^{z} dz'' \left\{ \frac{1}{\lambda_{cx}} + \frac{\nu_{ion}}{n_0} \frac{n_e(z'')}{\sqrt{v_z^2 - \frac{2e}{m_i}\left[\varphi(z') - \varphi(z'')\right]}} \right\}\right), \end{aligned} \tag{77}$$

where $\Delta(\xi) = 1$ at $\xi = 0$ and $\Delta(\xi) = 0$ for $\xi \neq 0$. The first term on the right-hand side of this equation defines the ion density at a single point in space $z_0(\to -\infty)$, where $\varphi(z_0) = 0$. It can therefore safely be dropped, since it does not contribute to the electric field. One can show that

$$J_i(z) = \nu_{ion} \int_{z_0}^{z} dz' n_e(z') \left[1 - \frac{n_i(z')}{n_0}\right], \tag{78}$$

which relates the ion flux to the ion and electron densities; this will be used in the numerical analysis of the problem.

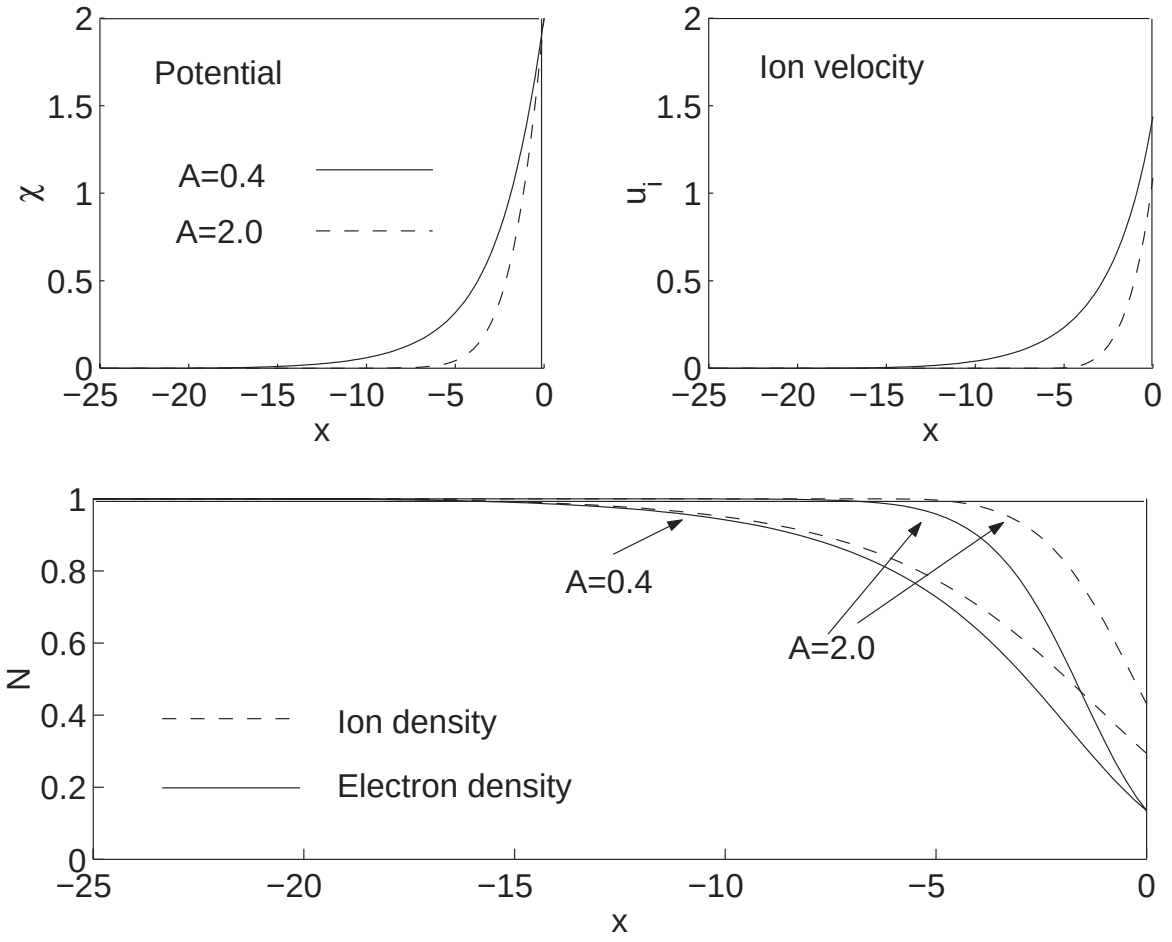

Figure 7: Normalized profiles of the potential (upper left panel), ion velocity $u_i = I_i/N_i$ normalized by c_s (upper right panel), and the electron and ion densities (lower panel), for $A = 0.4$ (solid lines) and $A = 2.0$ (dashed lines). For all cases $\lambda_{cx}/\lambda_D = 20$.

We now introduce the normalized (dimensionless) variables

$$x = \frac{z}{\lambda_D}, \quad \chi(x) = -\frac{e\varphi(z)}{T_e}, \quad N_i = \frac{n_i}{n_0}, \quad N_e = \frac{n_e}{n_0}, \quad J_i = n_0 c_s I_i, \tag{79}$$

and rewrite the Poisson Eq.(34) as

$$\frac{\partial^2 \chi}{\partial x^2} = N_i(x) - N_e(x), \tag{80}$$

where the electron and ion densities $N_e(x)$ and $N_i(x)$ are given by Eqs. (68), (77) and (79). Introducing the dimensionless variables into Eq.(78) and differentiating we obtain

$$N_i(x) = 1 - \frac{\sqrt{2}}{A N_e(x)} \frac{\partial I_i}{\partial x}, \tag{81}$$

so that Eq.(80) becomes

$$\frac{\partial^2 \chi}{\partial x^2} = 1 - N_e(x) - \frac{\sqrt{2}}{A N_e(x)} \frac{dI_i}{\partial x}, \tag{82}$$

where $N_e(x) = \exp[-\chi(x)]$ and

$$I_i(x) = \int_{x_0}^{x} dx' \left(\frac{\lambda_D}{\lambda_{cx}} I_i(x') + \frac{A}{\sqrt{2}} N_e(x') \right) \times \exp\left[-\frac{\lambda_D}{\lambda_{cx}}(x - x') - \frac{1}{2} A \int_{x'}^{x} dx'' \frac{N_e(x'')}{\sqrt{\chi(x'') - \chi(x')}} \right] . \quad (83)$$

By solving Eq. (82) we can find the normalized potential profile $\chi(x)$. In Eq. (83), which represents an integral equation for finding the dimensionless ion flux $I_i(x)$, the parameter

$$A = \sqrt{2} \frac{\nu_{ion} \lambda_D}{c_s} = \sqrt{2} \frac{\lambda_D}{\lambda_{ion}} \sqrt{\frac{m_i}{m_e}} \quad (84)$$

has been introduced.

10. Numerical results

In the numerical treatment, we solve the dimensionless Poisson equation (80) together with the following boundary conditions: $\partial\chi/\partial x = 0$ for $x = x_0 = -25$ (i.e., far away from the wall), and the potential on the wall ($x = 0$) is equal to $\chi = \chi_w = 2.0$. We use the normalized charge-exchange mfp $\lambda_{cx}/\lambda_D = 20$, while the ionization parameter A is varied.

The numerical results are displayed in Figs.7–9. In Fig.7 we considered the cases $A = 0.4$ and $A = 2.0$. We see that the scale length of the solution is longer for the lower ionization rate $A = 0.4$, with the boundary layer extending into the plasma. The splitting of electron and ion densities at the distance $|x| \approx 10$ for $A = 0.4$ and at the distance $|x| \approx 6$ for $A = 2.0$ is clearly seen. These distances can be considered as the width of the "sheath", while the distances $|x| > 10$ we can interpreted to be occupied by the "presheath". The ion velocity vanishes at increasing the distance from the wall. The point, where the ion velocity is equal to the ion-sound velocity, in our case does not indicate the sheath edge. For such a indication it is necessary to consider very small ratio $(\lambda_D/\lambda_{ion})$ (or very small values of the parameter A) [7].

We make a comparison between the theory presented here and recent experimental results carried out by Oksuz and Hershkowitz [6]. The experimental results are displayed in Fig.8 and our numerical results in Fig.9. In the numerical solution, we have used the same parameters as in the experimental setup and shifted the numerical solution so that a direct comparison can be made. In the experiment, the Debye radius was $\lambda_D = 0.25$ cm and the ion-neutral collisional mean-free-path was $\lambda_{cx} = 7.0$ cm, so that $\lambda_{cx}/\lambda_D = 28$; for the parameter A we used $A = 0.33$ (no values were given in the experiment). Furthermore, the electron temperature was 2.4 eV, yielding the relation $\varphi = -2.4\chi$ between the normalized potential χ and the potential φ given in Volts. In Fig. 9, we shifted the potential so that the potential of the bulk plasma was $2.5V$, similar as in the experiment displayed in Fig. 8. Panel (a) of Figs.8 and 9 show the whole plasma volume, where the solid line in Fig.9 indicates the numerical solution. In panel (b), we compare the potential obtained for the presheath in the experiment (Fig.8) and the numerical solution (Fig.9). We see that in the numerical solution, the potential connects smoothly to the bulk potential in a manner similar to what has been observed in experiments, while the theoretical fit indicated by the solid line in panel (b) of Fig.8 deviates strongly from the bulk plasma potential. This descrepancy is apparently due to the fact that the fit in question was based on a theory which, contratry to our present model, does not include recombination effect. In Fig.8(c) and 9(c) we compare the results for the transition region. Similar to the experimental results, we obtain the potential $1V$ at the position $z \approx -0.8$ cm, and $-5V$ at the position $z \approx 0.4$ cm, respectively. The experimental profile deviates slightly from the numerical one in that the experimental result exhibits a "knee" at the position 0 cm, not seen in the numerical solution. Fig.8(d) displays the measurement of the electron-free sheath, while the numerical solution is

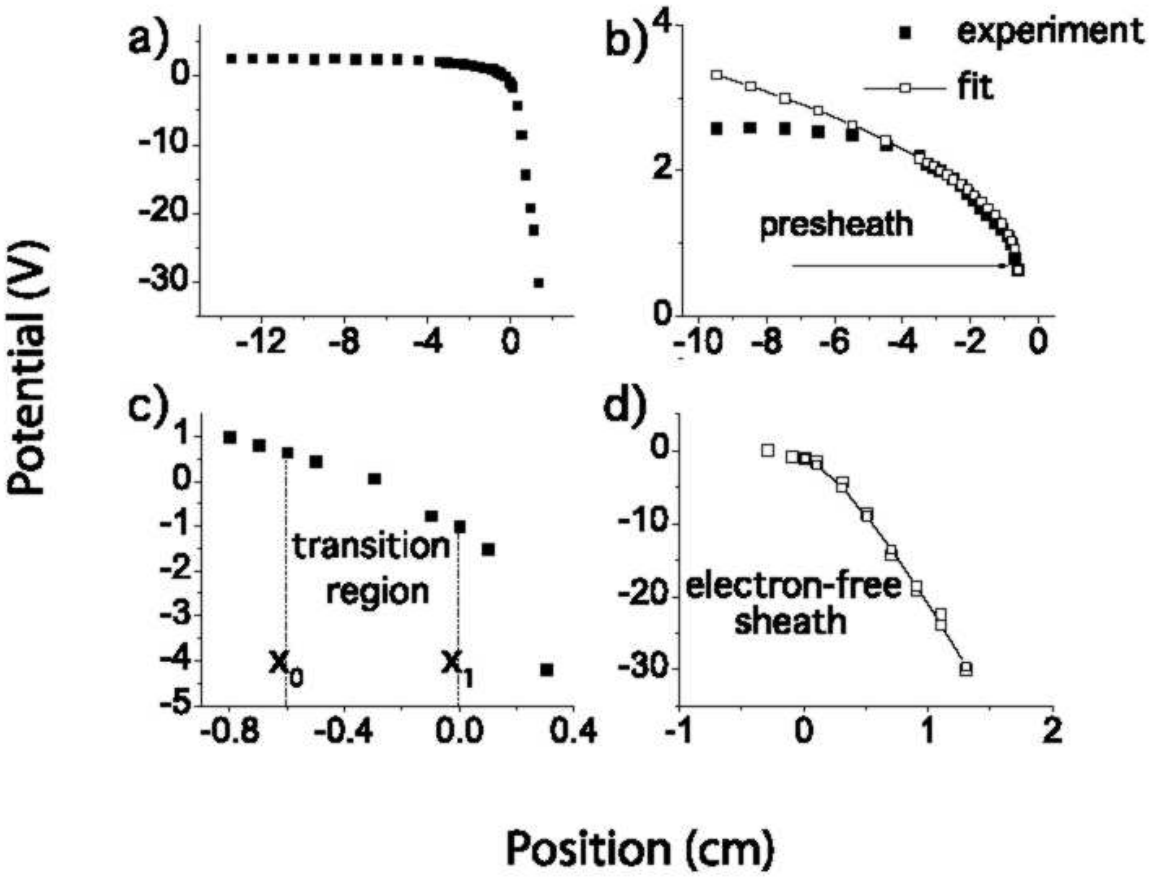

Figure 8: Experimental measurements of the electrostatic potential over (a) the whole plasma, (b) the presheath, (c) the transition region and (d) the electron-free sheath, all taken from the paper of *Oksuz and Hershkowitz* [6]. The filled squares are measured data while the lines show theoretical fits based on preaheath model by Riemann [7] [in (b)] and on the electron-free "Child-Langmuir sheath" [in (d)]

displayed in Fig.9(d). Due to convergence problems of the numerical solution, we were not able to cover the whole electron-free sheath, but we can still see that the values at the beginning of the electron-free sheath are approximately the same for the experiment and our numerical solution.

The numerical procedure used is as follows. The x space is divided into equidistant points $x_0, x_1, \ldots, x_M$, where x_0 is located at the edge $x = -L$ of the plasma-wall transition layer and x_M is located at the wall $x = 0$. The dependent variables are discretized so that $\chi(x_j) \approx \chi_j$, $N_e(x_j) \approx N_{e,j}$ and $I_i(x_j) \approx I_{i,,j}$. The second derivative of χ on the left-hand side and the first derivative of I_i on the right-hand side (82) are approximated with centered difference approximations. The resulting nonlinear system of equations for χ in Eq. (82), with fixed values for I_i, is solved iteratively by means of Newton iterations. For fixed values of χ, Eq. (83) is Fredholm's integral equation of second kind for unknown I_i. After the discretization, the integral equation is transformed to a linear system for the values in I_i, which is solved for I_i (by Gaussian elimination) to obtain the solution I_i'. The new value is set to $I_i^{new} = (1-\beta)I + \beta I_i'$, where β, is a parameter. This procedure is repeated until convergence, where β is chosen small enough (in the interval $0 < \beta \leq 1$) for convergence. The integral $I(x', x) = \int_{x'}^{x} dx'' N_e(x'')/\sqrt{\chi(x'') - \chi(x')}$ is approximated with the sum $I(x_m, x_n) \approx \sum_{k=m}^{n} \Delta x (N_{e,k-1} + N_{e,k})/(\sqrt{\chi_{k-1} - \chi_m} + \sqrt{\chi_k - \chi_m})$ with the step size $\Delta x = L/M$. The integration is exact when N_e is constant and χ is a linear function. The outer integral in Eq. (83) is approximated by the trapezoidal rule.

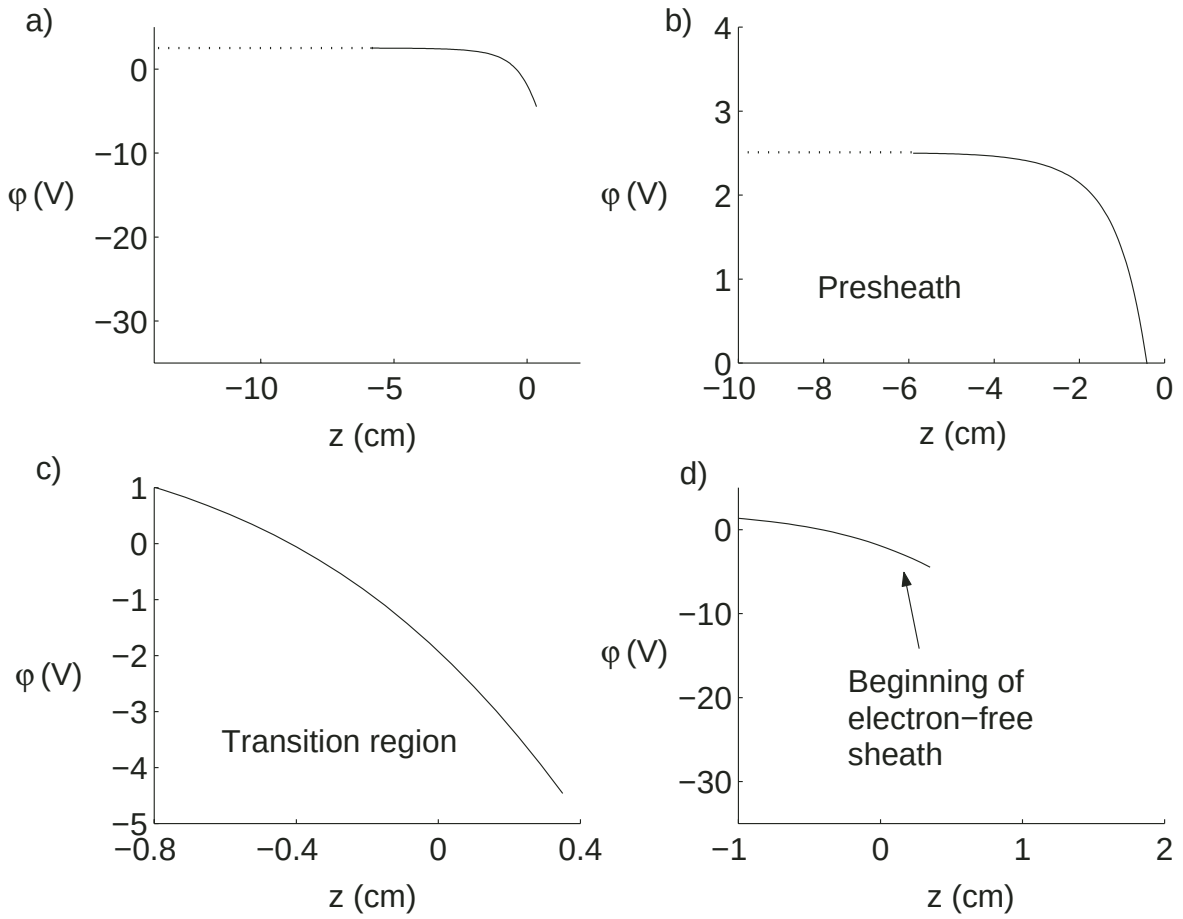

Figure 9: Numerical solution for the electrostatic potential over (a) over the whole plasma, (b) the presheath, (c) the transition region and (d) the electron-free sheath. The solid lines are our numerical results, while the dotted lines mark the potential 2.5 V of the bulk plasma. The origin of z-axis is shifted as in Ref. [6].

Acknowledgments

This work was supported by the Austrian Science Fund (FWF) through Projects P15013-N08 and P16807-N08, by the Deutsche Forschungsgemeinschaft through the Sonderforschungsbereich 591, and by the European Commission through the Association between EURATOM-ÖAW.

References

[1] I. Langmuir, Phys. Rev. **33**, 976 (1929).

[2] A. Caruso and A. Cavaliere, Nouovo Cim. **26**, 1389 (1962).

[3] R.N. Franklin and J.R. Ockendon, J. Plasma Physics 4, 371 (1970).

[4] G. Kino and E.W. Shaw, Phys. Fluids **9**, 587 (1966).

[5] K.-U. Riemann, Phys. D: Appl. Phys. **24**, 493 (1991).

[6] L. Oksuz and N. Hershkowitz, Phys. Rev. Lett. **89**, 145001 (2002).

[7] K.-U. Riemann, Phys. Plasmas **4**, 4158 (1997).

[8] N. Sternberg and V. Godyak, IEEE Trans. Plasma Sci. **31**, 665 (2003).

[9] R.N. Franklin, J. Phys. D: Appl. Phys. **36**, R309 (2003).

[10] R.N. Franklin, J. Phys. D: Appl. Phys. **37**, 1342 (2004).

[11] N. Sternberg and A.V. Godyak, IEEE Trans. Plasma Sci. **32**, 2271 (2004).

[12] L. Tonks and I. Langmuir, Phys. Rev. **34**, 876 (1929).

[13] D. Bohm, in "*The Characteristics of Electric Discharges in a Magnetic Field*", edited by A. Guthry and R.K. Wakerling (Mc Graw-Hill, New York, 1949

[14] K-U. Riemann, J. Tech. Phys. **41**, 89 (2000)

[15] E.M. Lifshitz and L.P. Pitaevskii, *Physical Kinetics* (Pergamon, Oxford, 1981), p.102.

[16] K.-U. Riemann, Phys. Fluids **25**, 2163 (1981).

[17] I.D. Kaganovich, Phys. Plasmas **9**, 4788 (2002).

[18] M. van Dyke, *Perturbation Methods in Fluid Mechanics* (Academic, New York, 1964).

[19] S. Kaplun, *Fluid Mechanics and Singular Perturbations* (Academic, New York, 1964).

[20] S. I. Braginskii, in *Reviews of Plasma Physics*, Vol. 1, edited by M. A. Leontovich, (Consultants Bureau, New York, 1964).

[21] M. Mitchner and C. H. Kruger, *Partially Ionized Gases* (John Wiley & Sons, New York, 1973).

[22] I. P. Shkarofsky, T. W. Johnston and M. P. Bachynski, *The Particle Kinetics of Plasmas* (Addison-Wesley, MA, 1966).

[23] U. Kortshagen, C. Bush and L.D. Tsendin, Plasma Sources Sci. Technol. **5**, 1 (1996).

[24] E.R. Harrison and W.B. Thompson, Proc. Phys. Soc. (London) **74**, 145 (1959).

[25] E.W. McDaniel and E.A. Mason, *The Mobility and Diffusion of Ions in Gases* (Wiley, New York, 1973), Chaps. 5, 6 and 7.

[26] F. F. Chen, *Plasma Physics and Controlled Fusion* (Plenum, New York, 1984), Vol.1, Chap.8.

[27] P. C. Stangeby, *The Plasma Boundary of Magnetic Fusion Devices* (IOP, Bristol, 2000), pp. 138-140.

[28] T. Holstein, J. Phys. Chem. **56**, 832 (1952).